Unusual pressure rise during the load rejection at a Deriaz turbine

IOP Conf. Series: Earth and Environmental Science **240** (2019) 022058 doi:10.1088/1755-1315/240/2/022058

Unusual pressure rise during the load rejection at a Deriaz turbine

H Kikuta[1], K Shimokawa[1], K Izutsu[1], T Tsukamoto[1] and S Nakamura[1]

[1] Voith Fuji Hydro K.K., Tanabeshinden, Kawasaki-ku, Kawasaki, 210-9830, Japan

hiroaki.kikuta@voith.com

Abstract. From the power generation optimization point of view, a type of Deriaz turbine was selected for the Y Hydropower Station in Japan, with the maximum net head of 60.7m and the rated output of 6.3MW. During the commissioning tests of the load rejection, unusual pressure rise waveforms were observed in the oscilloscope. The high frequency pressure fluctuations with large amplitude appeared on the water hammer pressure waveform. In most cases, the maximum pressure rise occurred at the peak of the pressure fluctuations and was close the guarantee. To mitigate the pressure fluctuation and have enough margins to the guarantee of the pressure rise, we tried various closing laws of the runner blade and guide vane and the aeration valve on and off. It is concluded that the pressure fluctuation was related to the developed swirl in the draft tube and there were two key factors to effectively mitigate the amplitude level at site. The one is to keep the closing law close to the on-cam relation during the load rejection. The second is to bring the guide vane opening as small as possible before the pressure fluctuations start, yet we have to take the balance with the water hammer pressure rise.

1. Introduction

Y Deriaz turbine hydropower station experienced the unusual pressure fluctuation during the commissioning tests of load rejection, quick shutdown and emergency shutdown.

Figure 1 (a) shows the unusual pressure fluctuation of Y Deriaz turbine during the load rejection and (b) shows a typical pressure rise waveform in a Francis turbine with a close specific speed of Y turbine. The Francis turbine only had the water hammer pressure rise waveform. Instead, the Y turbine had high frequency pressure fluctuation overlaid on the water hammer waveform. The detrimental pressure fluctuation was dominant to determine the maximum pressure rise and the peak to peak fluctuation amplitude reached 44% of the net head. The maximum pressure rise was under the guarantee of the penstock pressure. However, we were concerned about the result because the pressure rise converted from the tested head water level to the possible maximum head water level was close to the guarantee and the pressure fluctuation looked so stochastic that it seemed to possibly exceed the guarantee by chance. We decided to work on the mitigation of the pressure fluctuation by trying the various RV, GV closing law and the aeration valve on and off. In this paper, analysis methods are introduced and the results are presented and discussed.

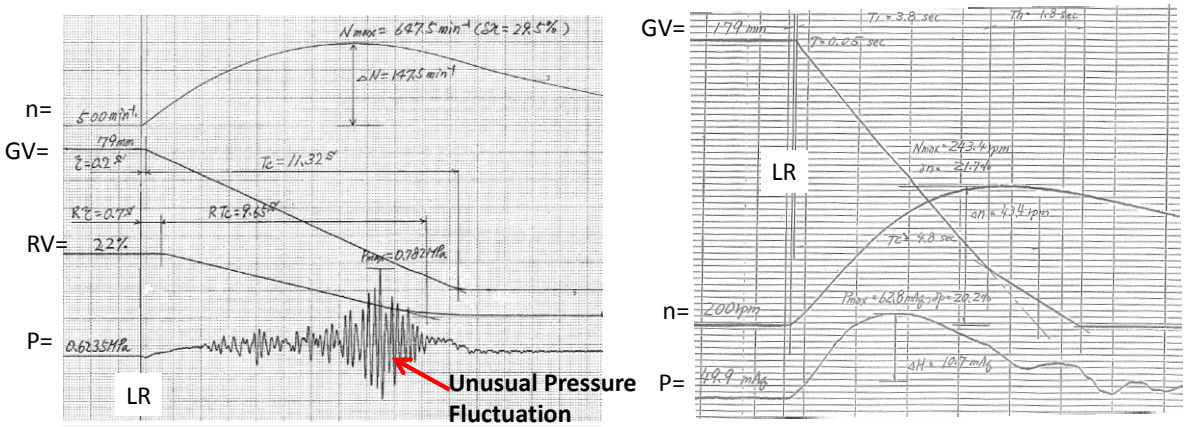

(a) Y Deriaz turbine: unusual pressure fluctuation during the load rejection

(b) Francis turbine (Nq~65) typical water hammer pressure rise

Figure 1. A Comparison of the pressure waveform during the load rejection.

2. Nomenclature

D_{ref}: reference diameter [m]
H: net head [m]
t: time [s]
GV: Guide Vanes
QS: Quick Shutdown
P: pressure in penstock [MPa] or [mAq]
$Nmax$: maximum speed rise [rpm] or [%]
n: generator speed [rpm] *[min^{-1}]= [rpm]
Q: discharge [m^3/s]
RV: Runner Vanes
LR: Load Rejection
HPS: Hydropower Station
$Pmax$: maximum pressure rise [MPa] or [mAq]
φ: RV opening [%] or [deg]

$n11$: unit speed, $n11 = \dfrac{n \cdot Dref}{\sqrt{H}}$

$Q11$: unit discharge, $Q11 = \dfrac{Q}{Dref^2 \sqrt{H}}$

u *and* U: local circumferential velocity, nominal circumferential velocity at the cross section
v *and* V: local axial velocity, nominal axial velocity at the cross section
α: flow angle, $\tan\alpha = U/V = m$

m: swirl intensity, $m = \dfrac{\int r \cdot v \cdot u \cdot dA}{\int r \cdot v^2 \cdot dA}$, where r: distance from the center, A: area of the cross section

$\Delta H/H$: peak to peak pressure fluctuation to the net head [%]

Nq: specific speed of the machine based on BEP, $Nq = n \cdot Q^{0.5} / H^{0.75}$

3. Y hydropower station

The specification of Y HPS is tabulated in Table 1. Figure 2 shows the Y HPS turbine cross section. To mitigate the up-thrust of RV during the load rejection, quick shutdown or emergency shutdown, a vacuum breaker feeding the air is installed between GV and RV. To break the vortex rope causing the pressure pulsation during the normal part load operation, a forced air system of a jet pump, pushing air with the penstock water, was installed. As the turbine has 8 blades, the blades contact the adjacent blade at 25% output. Under that output, the turbine operates at off-cam relation, causing a rough

operation with the pressure pulsation. To achieve the smooth operation even under off-cam condition, the forced air system was applied.

Table 1. Specification of Y hydropower station.

Max discharge	[m3/s]	13
Max net head	[m]	60.7
Rated net head	[m]	56.0
Synchronous speed	[rpm]	500
Generator output	[kW]	6300
Number of blade	[-]	8
Specific speed (Nq)	[-]	71

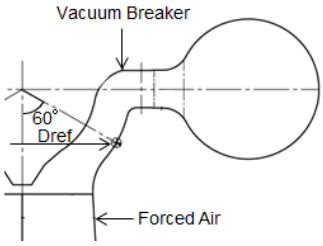

Figure 2. Y HPS Deriaz turbine cross section view.

4. Understanding of the unusual pressure fluctuation

4.1. Water hammer simulation

In advance of the commissioning test, the water hammer simulation based upon the characteristic curve method was performed. Figure 3 shows the result. In the pressure rise waveform, there is no high frequency pressure fluctuation. Therefore the pressure fluctuation is not a nature from water hammer phenomena.

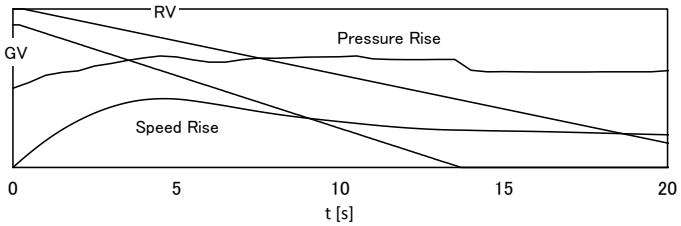

Figure 3. Result of water hammer simulation for Y HPS 100% load rejection.

4.2. Water conduit resonance check

Also the possibility of the water conduit resonance was simply checked. The pressure fluctuation frequency measured at site was around 3-5 Hz (Table 2). Instead the natural frequency of the 1st elastic mode of water conduit (=Speed of sound/water conduit length/4) was 2Hz or lower. So the pressure fluctuation was not the result of this kind of resonance.

4.3. High frequency pressure fluctuation in other types of machines

During the high-head pump-turbines load rejection, it is well known that the high frequency fluctuation is observed in the vaneless space with the rotor-stator interaction. The frequency is related to n*Zr, where n: rotational speed and Zr: number of blade. For Y HPS, this frequency was calculated and it was 65Hz or more, which does not match the measured frequency.

In a Bulb turbine, a singular pressure variation during the load rejection was reported by Yamato [1]. The pressure variation was related to the air content remaining as gas in the turbine. During the load rejection, the void fraction in the water changes a lot thus the speed of sound drastically changes, resulting in the singular pressure variations. The authors also experienced this phenomenon recently in the other Bulb turbine. Figure 4 shows the results. When the Bulb runner was replaced, the vacuum breaker was additionally installed. After the vacuum breaker was installed, the additional pressure fluctuation was present during the quick shutdown (and load rejection). We have concluded that the pressure fluctuation was caused by the air content change during the load rejection in a similar mechanism of [1].

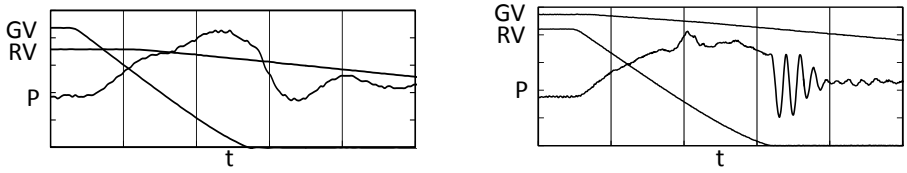

(a) without vacuum breaker (b) with vacuum breaker

Figure 4. Bulb turbine pressure fluctuation during quick shutdown.

Y HPS also has the vacuum breaker feeding the air during the load rejections. However, this mechanism of the fluctuation is not the case for 60m net head Deriaz turbine. In the singular pressure variation observed in the low head Bulb turbines (16m or lower), enough amount of air should remain as gas to change the void fraction much. However, in Y HPS with the net head of 60m, the void fraction change should be limited because of the high pressure in the water and thus the low void fraction change. Also, in another 100m Deriaz turbine without the vacuum breaker, we also have seen the pressure fluctuation similar to the one observed in Y HPS. Therefore, the air fed through the vacuum breaker is not the decisive factor of the pressure fluctuation.

In Francis turbines, it is widely accepted that the part load pressure pulsation was caused by the rough behaviour of vortex rope and its frequency is about 0.2-0.4 times of the shaft rotation frequency. The frequency of the pressure fluctuation in Y HPS was within the range of this (Table 2). Therefore, it can be assumed that the vortex rope in the draft tube causes the pressure fluctuation.

4.4. High frequency pressure fluctuation in other Deriaz turbines

In fact, in some Deriaz turbines, the authors also experienced the pressure fluctuations similar to the one in Y HPS. Figure 5 shows the one of the examples in a Deriaz pump-turbine load rejection. The pressure fluctuation with high amplitude and high frequency was observed, thus we adjusted the closing law of RV to mitigate it. By shortening the RV closing time, the fluctuation was completely removed. The strategy taken in this case was to try to keep the on-cam as much as possible during the load rejection, avoiding the vortex rope development in the draft tube. It was successful.

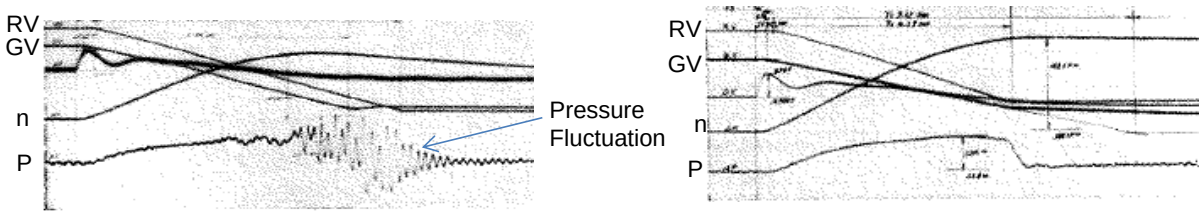

(a) original RV closing time (b) RV closing time adjusted

Figure 5. A Deriaz pump-turbine load rejection oscillograph.

In the model test for a Deriaz turbine project (Nq~55, number of RV=10), not for Y HPS, the behaviors of pressure fluctuation was investigated for a wide n11 range. Figure 6 shows the pressure fluctuation percentage in net head at three combinations of RV/GV openings. Looking at Figure 6 (a), the smoothest condition was at on-cam for all RV/GV openings. The pressure fluctuation *ΔH/H* went higher so quickly as n11 increased. At around runaway condition, *ΔH/H* reached its peak and beyond that point *ΔH/H* fell down. *ΔH/H* tended to be higher at the draft tube than spiral case inlet, which strongly indicated the fluctuation was caused by the draft tube vortex rope. Figure 6 (b) shows the effect of aeration from the draft tube side wall with 1% air to the rated water flow rate. Because the origin of the fluctuation was the vortex rope, by feeding the air the rope was broken and the flow in the turbine became smoother.

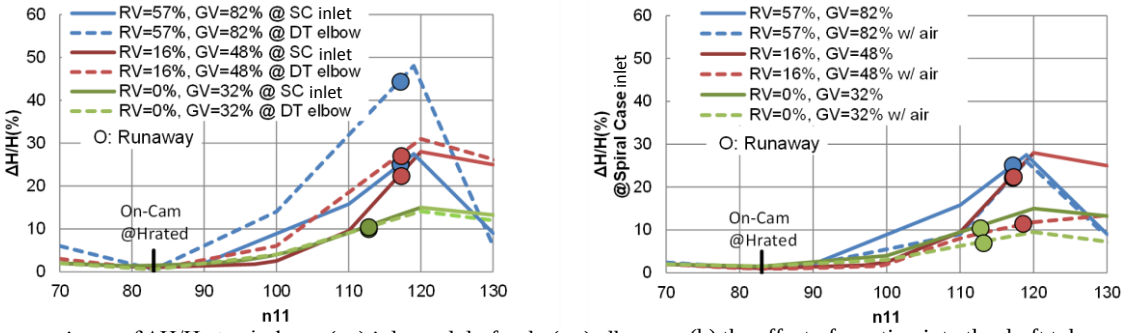

(a) comparisons of ΔH/H at spiral case(SC) inlet and draft tube(DT) elbow (b) the effect of aeration into the draft tube

Figure 6. A Deriaz turbine (Nq~55) pressure fluctuation in the model test.

Showing the two cases of the Deriaz turbine pressure fluctuation, the origin of the pressure fluctuation observed in Y HPS was also related to the draft tube whirl flow with the vortex rope.

For Y HPS, hints of the possible strategies for the pressure fluctuation reduction during the load rejection/quick shutdown are indicated based on Figure 6. Seeing the results, up to the runaway speed, the farther an operating point goes away from the on-cam relation, the higher the pressure fluctuation becomes and the higher the turbine discharge (RV,GV opening) goes, the higher the pressure fluctuation becomes. Therefore, to mitigate the pressure fluctuation, (1) keep the RV/GV relation close to on-cam throughout the transient process and (2) before reaching the runaway, we should reduce the flow as much as possible. Also the air injection seems to be effective.

5. Analysis methods

5.1. Pressure Fluctuation

To clarify the behaviors of the high frequency pressure fluctuation, a method of extracting the component is presented here. Figure 7 (a) shows the typical pressure rise waveform of Y HPS during the load rejection. When looking at the waveform, it is naturally noticed that the waveform is composed of two parts, one is the high frequency pressure fluctuation and the rest of the component, which should be related to the water hammer pressure rise. Figure 7(b) shows the decomposed waveforms from the original one of Figure 7. First, the high frequency waveform was extracted such that its frequency is higher than round-trip frequency of the water hammer (around 2Hz) and the pressure fluctuation component is obtained as seen in Figure 7(b) (purple). Then the rest of the component is obtained as the water hammer waveform (green).

With this decomposition method, the time dependent behaviors of the pressure fluctuation and water hammer waveform are obtained.

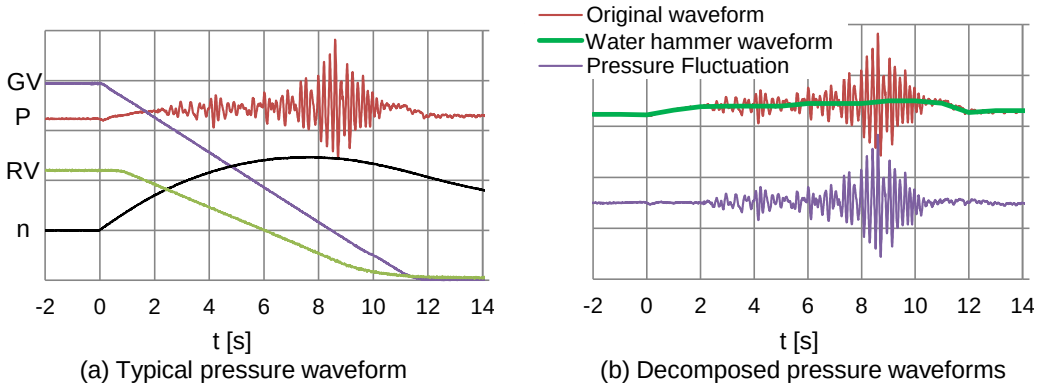

Figure 7. Typical pressure rise waveform and the decompositions (Test-a).

5.2. φ-n11/Q11 chart and the flow angle at the draft tube inlet

In the previous sections, the high amplitude pressure fluctuation is considered to be related to the draft tube vortex rope. The authors, at the beginning, tried to show the flow angle α at the inlet of the draft tube because it is the key parameter to describe the development of the draft tube vortex rope [2] (swirl intensity m=tanα) causing the pressure fluctuation. However, it is hard to get the actual flow angle during the transient process by the CFD, the model test or the site test in the prototype machine.

Instead of directly showing flow angles, a simple 2D *φ-n11/Q11* chart is introduced to show how far the operating point of interest (*n11, Q11, φ, t*) is from the on-cam state, assuming the flow angle is low at on-cam and the higher at the farther point from the on-cam. Based on the model tested data, we had data set of *n11, Q11* and *φ* at on-cam relation in the wide range. When 17 pairs of *φ-n11/Q11* at on-cam are plotted, they are well collected and make one curve. Figure 8 shows the result of Y HPS. Because on-cam state is expressed on the *φ-n11/Q11* chart as one curve regardless of *n11*, this is useful to simply show the state of the operating points, for example, A is at on-cam (on the on-cam curve), B at strong off-cam (far above the on-cam curve) or C at weak off-cam (not on the on-cam curve but near).

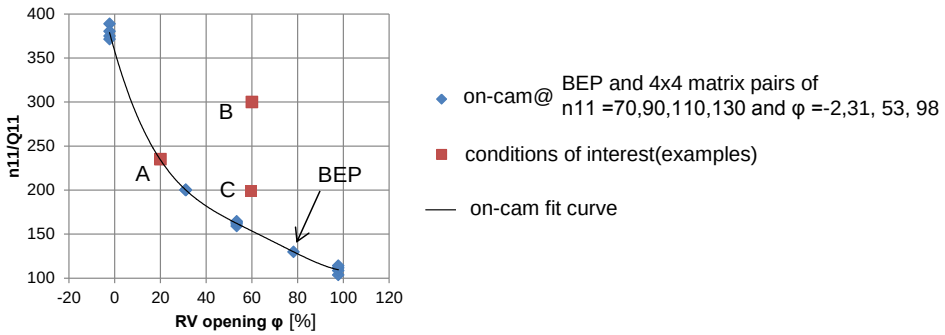

Figure 8. *φ-n11/Q11* chart.

The reason is discussed here why on-cam relations of (*φ, n11/Q11*) are well-collected on one curve. Looking at the model tested data (not shown in this paper), throughout wide n11 range from 70 to 130 at constant RV opening, *n11/Q11* values at on-cam was almost constant. When the RV opening varies, the on-cam *n11/Q11* value also varies. This is the direct reason.

To briefly understand the physics behind the reason, the simplified velocity triangle at the RV discharge is shown in Figure 9. It is known that *n11* is related to the circumferential velocity *U* and

Q11 to the axial velocity *V*. Therefore, the flow angle α in the absolute coordinate system is geometrically expressed with the parameters of *φ, n11/Q11*. Throughout the wide *n11* range, the on-cam was found at the constant *φ* and *n11/Q11* thus the constant flow angle and this indicates that the on-cam condition strongly depends on the flow angle at the inlet of the draft tube (at the discharge of the RV). It can be also said that the farther the operating point goes away above the on-cam curve in the chart, the higher the flow angle becomes.

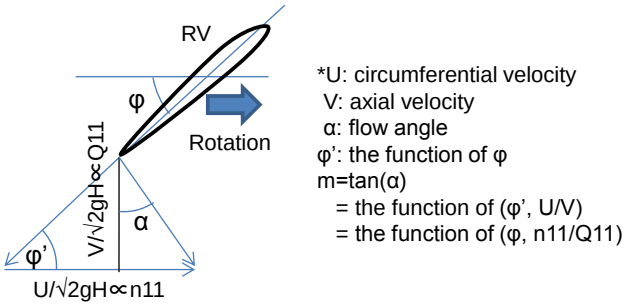

Figure 9. Simplified velocity triangle at the discharge and *φ-n11/Q11*.

However, the limit of *φ-n11/Q11* chart interpretation for this purpose should be taken into account. Firstly, the distance of the operating point from on-cam curve does not directly give the flow angle. At on-cam, it tends to have non-zero flow angle and it varies depending on the flow rate [3]. Secondary, the flow angle was derived from the simplified velocity triangle. In the actual flow, the more complicated flow is formed for example with secondary flow. Thirdly, even if the operating point of interest is at the same distance from on-cam curve at the same *φ* in the chart, interpreting the same level of the flow angle, the actual development of the vortex rope could be affected by the transient process, for example, time delay of the vortex formation or the time dependent route of *n11, Q11*.

Nevertheless, authors believe that using the *φ-n11/Q11* chart helps a good guess to know the flow state in the draft tube and gives graphical understandings in a simple way. The *φ-n11/Q11* chart of Figure 10 shows the 17 cases of load rejections / quick shutdown tested with various RV/GV closing laws in Y HPS. In the chart, each case of the normal operation point before the LR/QS, the high frequency pressure fluctuation starting point, the point reaching maximum pressure fluctuation and the trajectory are shown. From the results, in various closing laws, it seems that the distances from the on-cam curve are found with a certain tendency for the pressure fluctuation starting points and the maximum fluctuation points. This indicates that one of the key factors of the pressure fluctuation is again the flow angle at the draft tube inlet and *φ-n11/Q11* chart works for the investigation purpose of the flow state causing the pressure fluctuation.

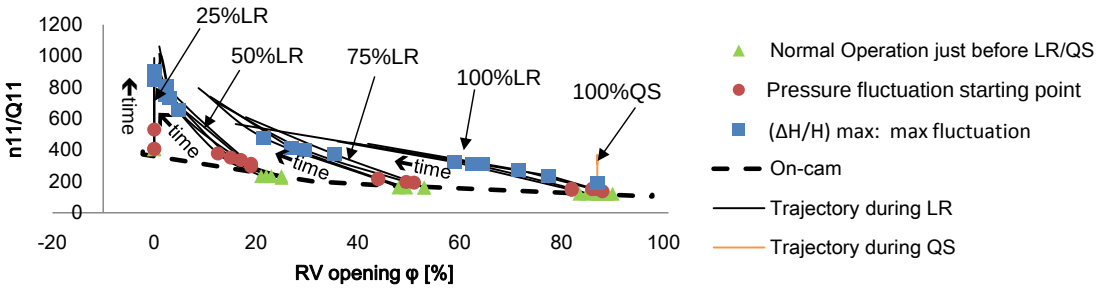

Figure 10. *φ-n11/Q11* chart of 17 cases of load rejections/quick shutdown in Y HPS.

6. Results and discussions

6.1. Test cases and overview of the results

More than 40 tests of the load rejection, quick shutdown and emergency shutdown were performed to find the way to best mitigate the pressure fluctuation by changing the RV/GV closing laws and aeration on/off. The important test cases and results are shown in Table 2. In the table, to show the effects of the measures taken clearly, the test cases are separated in five groups. Details for each group are shown after this section.

Table 2. Test cases and Results.

Test condition						Comparison		Result			
Test ID	Load	Type	Aeration	Closing time [s]		Group	Description	Pmax [MPa]	Nmax [rpm]	ΔH/H max [%]	Dominant Freq. [Hz]
				GV	RV						
a	50%	Load Rejection	w/o air	21.7	42.0	a-b-c	Closing time: org setting	0.782	647.5	44	4-5
b	50%	Load Rejection	w/o air	30.0	23.3	a-b-c	Closing time: RV fastest	0.754	679.0	37	4-5
c	50%	Load Rejection	w/o air	13.5	23.3	a-b-c c-d	Closing time: GV,RV fastest Aeration	0.698	604.0	14	4-5
d	50%	Load Rejection	w/ air	13.5	23.3	c-d	Aeration	0.738	608.0	21	4-5
e	100%	Load Rejection	w/o air	21.7	42.0	e-f	Closing time: org setting	0.742	695.0	26	4-5
f	100%	Load Rejection	w/o air	13.5	23.3	e-f f-g	Closing time: GV,RV fastest Aeration	0.713	680.0	17	4-5
g	100%	Load Rejection	w/ air	13.5	23.3	f-g	Aeration	0.706	685.0	14	4-5
h	100%	Qick Shutdown	w/o air	13.5	23.3	h-i	Close RV	0.756	500.0	32	3-4
i	100%	Qick Shutdown	w/o air	13.5	–	h-i	Keep RV	0.708	500.0	19	3-4

6.2. RV/GV closing law effect at 50% load rejection: Group a-b-c

To investigate the effect of RV/GV closing law at 50% load rejection, 3 cases of Test-a, b, c were performed. Figure 11(a) shows *φ-n11/Q11* chart and (b) shows *n11-Q11* trajectory with the pressure fluctuation amplitude at every one second (each circle diameter shows the *ΔH/H* %). The *n11, Q11* were determined with the RV/GV opening and the decomposed water hammer pressure (for net head), referring to the model tested relations. The Test-a was the original setting of the closing law, resulting in the largest *Pmax* as shown in Table 2. For the mitigation, our strategy taken was to keep the on-cam as much as possible. In Test-b, we set RV the fastest and GV very slow. In Figure 11(a), just after the load was rejected, Test-b was the closest to the on-cam as expected. However, the trajectory quickly went farther from the on-cam and reached max *ΔH/H* at high *n11/Q11*. Because GV was closed slowly, the runner speed rose the highest and at near *φ*=0%, *n11/Q11* had to become high. This might be one of the reasons that the reduction of *ΔH/H* was limited (44 to 37%). On the contrary, in Test-c, the fastest GV closing was tried and it achieved a large *ΔH/H* reduction (44 to 14%). In Test-a, we could make the trajectory closer to the on-cam and at the same time could keep the speed lower. Even taking into account the water hammer pressure rise increase by the fast closing GV, the total pressure-rise was well reduced.

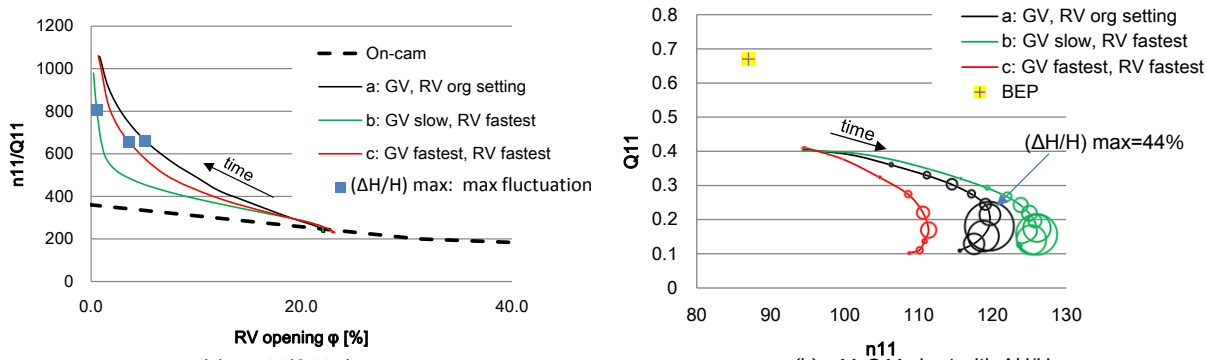

(a) *φ-n11/Q11* chart (b) *n11-Q11* chart with ΔH/H

Figure 11. Group a-b-c, 50% load rejection varying the RV/GV closing law.

6.3. RV/GV closing law effect at 100% load rejection: Group e-f

To investigate the effect of RV/GV closing law at 100% load rejection, 2 cases of Test-e, f were performed. Figure 12(a) shows *φ-n11/Q11* chart and (b) shows *n11-Q11* trajectory with the pressure fluctuation amplitude at every one second. The Test-e was the original setting of the closing law, resulting in the larger *Pmax* as shown in Table 2. For the mitigation, our strategy taken was to use the same measure as Test-a, b, c, the fastest RV/GV closing. It successfully worked for the reduction of *ΔH/H* from 26 to 17% and *Pmax*.

In Figure 12(a), the trajectories on the *φ-n11/Q11* chart coincided with each other by chance. Thus it can be taken as the same flow angles in both cases. What made different in *ΔH/H* was *n11, Q11* trajectories in Figure 12(b). The pressure fluctuation became the highest around the runaway speed, where the speed turned to deceleration (See also Figure 6 and Figure 11(b)). Test-f passed the runaway at the lower flow rate, so the energy of water into the vortex rope was lower. This could be one of the reasons why Test-f showed lower *ΔH/H*.

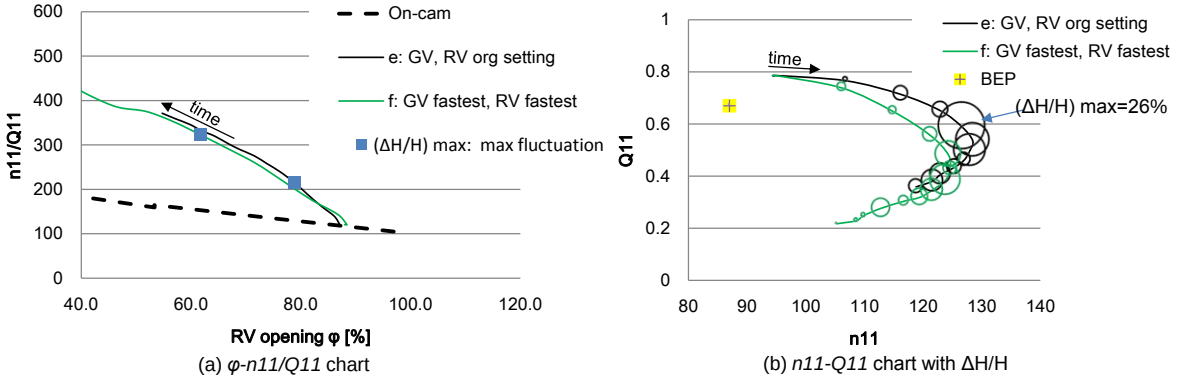

(a) *φ-n11/Q11* chart (b) *n11-Q11* chart with ΔH/H

Figure 12. Group e-f, 100% load rejection varying the RV/GV closing law.

6.4. Aeration on/off effect, Group c-d, f-g

To investigate the effect of the forced aeration from the draft tube side wall, 2 cases of Test-c, d were performed. According to the other project of the Deriaz turbine model test shown in Figure 6, the aeration should be useful to reduce the pressure fluctuation. At 100% load rejection for Test-f and g, the aeration helped the reduction of the pressure fluctuation from 17 to 14% as shown in Table 2. On the other hand, at 50% load rejection for Test-c and d, the pressure fluctuation *ΔH/H* was increased from 14 to 21%. Before the load rejection, the aeration valve was closed to avoid the performance

reduction and once the load was rejected, it simultaneously started opening the valve. Actually, it takes 13 seconds to fully open the aeration valve. Therefore, in this condition, it seemed that air injection was not enough to break the vortex rope. As a reference, in Figure 13, the model test result of the aeration effect to *ΔH/H* is shown for the case of an Nq~65 Francis machine. At a certain load, *ΔH/H* was higher at 1% air than no air condition. When the air reached 2%, a reduction in *ΔH/H* was found. It seemed that the vortex rope in the draft tube was destabilized by the air at 1%, instead. From this, it can be assumed that insufficient air injection could lead an increase of pressure fluctuation.

Based on the result at site in Y HPS, we decided to not open the air valve when the load is rejected.

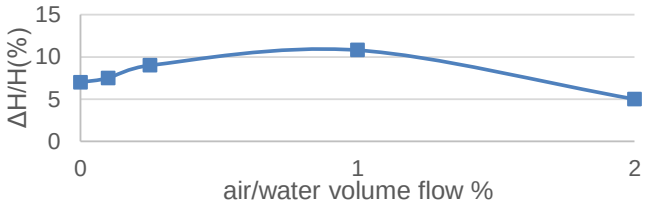

Figure 13. Aeration effect at 70% load in Nq~65 Francis turbine.

6.5. Close / keep RV during 100% quick shutdown, Group h-i

To investigate the effect of the RV opening during the quick shutdown, 2 cases of Test-h, i were performed. During the quick shutdown from t=0 to t=11, the runner speed was kept at 500 rpm. Figure 14 (a) shows *φ-n11/Q11* chart and (b) shows *t-n11, Q11* trajectory with the pressure fluctuation amplitude at every one second on the *t-Q11* curve.

Based on the result, it is found that keeping the RV/GV openings close to the on-cam is not always true for the mitigation of the pressure fluctuation *ΔH/H*. Figure 14 (b) shows that during the quick shutdown, both cases of the trajectory on *n11, Q11* were almost same. Therefore, closing the RV during the process should be more ideal to keep the flow state close to the on-cam. However, Test-i, keeping the RV, resulted in the lower pressure fluctuation.

Unfortunately, we did not find the reason for this phenomenon. There might be a range of parameters, the flow angle and the flow rate, where the vortex rope in the draft tube largely oscillates.

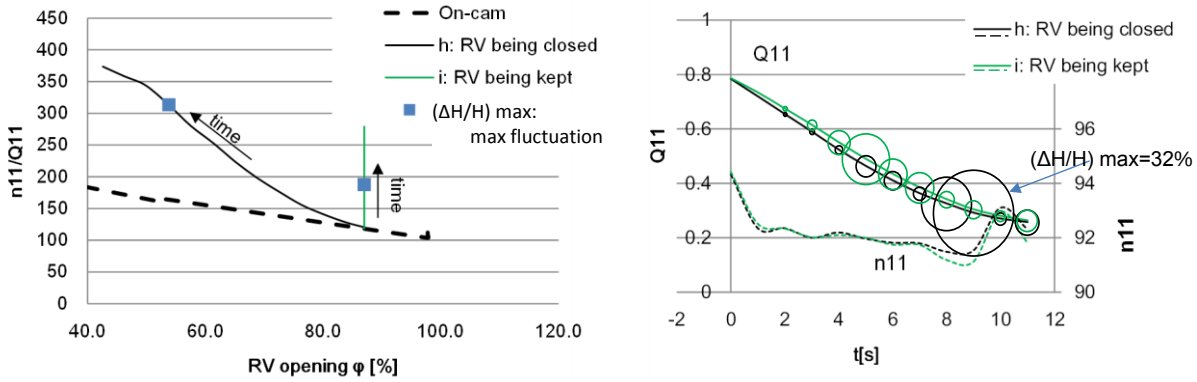

(a) *φ-n11/Q11* chart (b) *t-n11,Q11* with ΔH/H

Figure 14. Group h-i, 100% quick shutdown, keeping RV open / closing RV.

7. Conclusion

In Y HPS, the unusual pressure rise with high frequency pressure fluctuation was observed during the load rejection / quick shutdown. The peak to peak pressure fluctuation amplitude reached 44% of the net head and it was dominant to determine the maximum pressure rise. To mitigate the pressure fluctuation, more than 40 cases with various RV / GV closing laws and aeration on/off were tried at site. The investigations are summarized as follows.

(1) In the water hammer simulation, the pressure fluctuation was not observed. This showed that the high frequency pressure fluctuation was not caused by the water hammer effect.
(2) The possibilities of the water conduit resonance, the rotor-stator interaction and the fluctuation caused by the remaining air as gas in the water were investigated. It has been found that the pressure fluctuation observed in Y hydropower station was not any of the cases.
(3) It has been found that the pressure fluctuation frequency was within a typical range of the part load vortex rope oscillation.
(4) In some Deriaz turbines, the pressure fluctuation similar to the one in Y hydropower station was found. Considering the counter measure taken to suppress the fluctuation in a Deriaz pump-turbine and the model tested data for an Nq~55 Deriaz turbine, the assumption was more supported that the pressure fluctuation observed in Y Deriaz turbine was caused by the rough vortex rope flow in the draft tube. In addition, based on Nq~55 Deriaz turbine data (Figure 6), the strategies for the reduction of pressure fluctuation were indicated.
(5) To understand the phenomena during the transient process of load rejection and quick shutdown in Y hydropower station, an analysis method for the decomposition of waveform into high frequency fluctuation part and water hammer pressure rise part was introduced. Also the *φ-n11/Q11* chart was introduced to graphically understand the flow state at the draft tube inlet, indirectly showing the flow angle. The usage/interpretation of the *φ-n11/Q11* chart and the limit of the usage were discussed.
(6) Comparison tests with different RV/GV closing laws were performed during the 50% and 100% load rejections. The successful strategies were keeping the RV close to on-cam and controlling the speed rise and flow rate before reaching the maximum pressure fluctuation. It has also been noticed that the maximum pressure fluctuation tended to occur near the runaway condition (around the maximum speed rise). For the case of Y Deriaz turbine, water hammer pressure rise was not dominant, so closing RV/GV in the fastest speed was successful. However, the water hammer effect should be accordingly taken care of depending on cases.
(7) Comparison tests with the aeration on/off during the load rejection were performed. According to the laboratory model test for an Nq~55 Deriaz turbine project, the aeration was useful to break up the vortex rope and mitigate the pressure fluctuation. However, in Y Deriaz turbine, aeration was not a universal solution because of the time delay of the aeration valve opening.
(8) Comparison tests with the RV being kept or being closed during the quick shutdown were performed. Unexpectedly, it has been found that keeping the RV openings close to the on-cam was not always true for the mitigation of the pressure fluctuation.

In this paper, the authors reported the comparisons of the pressure fluctuation for various RV/GV closing laws and showed time-dependent changes in some dominant parameters, such as on-cam/off-cam, flow rate and net head, to find hints for the reduction of the pressure fluctuation. As we had kind suggestions from some researchers during/after IAHR2018 symposium in Kyoto, the physics behind the phenomena will be more focused on for the future work considering the detailed flow field and the flow system.

Acknowledgements
Authors wish to acknowledge supports and insightful advices from Dr. Yamato, Shoichi in Fuji Electric.

References
[1] Yamato S, Shimokawa K, Nakamura S and Nakai M 2017 *Proc. Hydro2017* Relationship between wave propagation velocity and singular pressure variation at load rejection
[2] Nishi M, Matsunaga S, Kubota T and Senoo Y 1982 *Proc. IAHR 11th Symp* Flow regimes in an elbow-type draft tube Vol. 2, pp. 38/1-13
[3] Nakamura S, Yamato S and Furukawa A 2010 *Proc. Renewable Energy 2010* Experimental study of draft tube performance in bulb turbine O-Sh-4-4